



# Maternal *GNAS* Contributes to the Extra-Large G Protein $\alpha$ -Subunit (XL $\alpha$ s) Expression in a Cell Type-Specific Manner

Quixia Cui<sup>1,2</sup>, Cagri Aksu<sup>1</sup>, Birol Ay<sup>1</sup>, Claire E. Remillard<sup>1</sup>, Antonius Plagge<sup>3</sup>, Mina Gardezi<sup>4</sup>, Margaret Dunlap<sup>4</sup>, Louis C. Gerstenfeld<sup>4</sup>, Qing He<sup>1,5</sup> and Murat Bastepe<sup>1\*</sup>

<sup>1</sup> Endocrine Unit, Department of Medicine, Massachusetts General Hospital and Harvard Medical School, Boston, MA, United States, <sup>2</sup> Department of Thyroid and Breast Surgery, Zhongnan Hospital of Wuhan University, Wuhan, China, <sup>3</sup> Department of Molecular Physiology and Cell Signalling, Institute of Systems, Molecular and Integrative Biology, University of Liverpool, Liverpool, United Kingdom, <sup>4</sup> Department of Orthopaedic Surgery, Boston University School of Medicine, Boston, MA, United States, <sup>5</sup> School of Stomatology, Wuhan University, Wuhan, China

## OPEN ACCESS

### Edited by:

Aleksander Jamsheer,  
Poznan University of Medical  
Sciences, Poland

### Reviewed by:

Serap Demircioglu Turan,  
Marmara University, Turkey  
Guiomar Perez De Nanclares,  
Osakidetza Basque Health Service,  
Spain

### \*Correspondence:

Murat Bastepe  
bastepe@helix.mgh.harvard.edu

### Specialty section:

This article was submitted to  
Genetics of Common and Rare  
Diseases,  
a section of the journal  
Frontiers in Genetics

Received: 14 March 2021

Accepted: 12 May 2021

Published: 17 June 2021

### Citation:

Cui Q, Aksu C, Ay B,  
Remillard CE, Plagge A, Gardezi M,  
Dunlap M, Gerstenfeld LC, He Q and  
Bastepe M (2021) Maternal *GNAS*  
Contributes to the Extra-Large G  
Protein  $\alpha$ -Subunit (XL $\alpha$ s) Expression  
in a Cell Type-Specific Manner.  
*Front. Genet.* 12:680537.  
doi: 10.3389/fgene.2021.680537

*GNAS* encodes the stimulatory G protein alpha-subunit (G $\alpha$ ) and its large variant XL $\alpha$ s. Studies have suggested that XL $\alpha$ s is expressed exclusively paternally. Thus, XL $\alpha$ s deficiency is considered to be responsible for certain findings in patients with paternal *GNAS* mutations, such as pseudo-pseudohypoparathyroidism, and the phenotypes associated with maternal uniparental disomy of chromosome 20, which comprises *GNAS*. However, a study of bone marrow stromal cells (BMSC) suggested that XL $\alpha$ s could be biallelically expressed. Aberrant BMSC differentiation due to constitutively activating *GNAS* mutations affecting both G $\alpha$  and XL $\alpha$ s is the underlying pathology in fibrous dysplasia of bone. To investigate allelic XL $\alpha$ s expression, we employed next-generation sequencing and a polymorphism common to XL $\alpha$ s and G $\alpha$ , as well as A/B, another paternally expressed *GNAS* transcript. In mouse BMSCs, G $\alpha$  transcripts were 48.4  $\pm$  0.3% paternal, while A/B was 99.8  $\pm$  0.2% paternal. In contrast, XL $\alpha$ s expression varied among different samples, paternal contribution ranging from 43.0 to 99.9%. Sample-to-sample variation in paternal XL $\alpha$ s expression was also detected in bone (83.7–99.6%) and cerebellum (83.8 to 100%) but not in cultured calvarial osteoblasts (99.1  $\pm$  0.1%). Osteoblastic differentiation of BMSCs shifted the paternal XL $\alpha$ s expression from 83.9  $\pm$  1.5% at baseline to 97.2  $\pm$  1.1%. In two human BMSC samples grown under osteoinductive conditions, XL $\alpha$ s expression was also predominantly monoallelic (91.3 or 99.6%). Thus, the maternal *GNAS* contributes significantly to XL $\alpha$ s expression in BMSCs but not osteoblasts. Altered XL $\alpha$ s activity may thus occur in certain cell types irrespective of the parental origin of a *GNAS* defect.

**Keywords:** *GNAS*, stimulatory G protein, imprinting, osteoblasts, bone marrow stromal cells, fibrous dysplasia of bone

## INTRODUCTION

*GNAS* is an imprinted gene encoding the alpha-subunit of the stimulatory G protein (G $\alpha$ ), a signaling protein mediating the actions of many endogenous molecules via generation of cAMP (Plagge et al., 2008; Weinstein et al., 2004; Mantovani et al., 2016). Loss-of-function mutations or epigenetic alterations of *GNAS* are responsible for different human diseases that involve abnormal skeletal development, metabolism, and hormone actions, such as pseudohypoparathyroidism Ia (MIM: 103580). Gain-of-function *GNAS* mutations affecting the activity of G $\alpha$  are found in a variety of benign and malignant tumors, as well as in patients with fibrous dysplasia of bone and McCune-Albright syndrome (MIM: 174800). *GNAS* gives rise to multiple additional products showing exclusively maternal or paternal expression (Bastepe, 2007; Kelsey, 2010). The extra-large G-alpha subunit (XL $\alpha$ s) is a variant of G $\alpha$  that uses a separate promoter and a unique first exon that splices onto G $\alpha$  exon 2 (Kehlenbach et al., 1994; Hayward et al., 1998). Hence, XL $\alpha$ s is partly identical to G $\alpha$  and can mimic the latter regarding cAMP generation (Klemke et al., 2000; Bastepe et al., 2002); however, XL $\alpha$ s mediates additional cellular actions, such as stimulation of IP3/PKC signaling and inhibition of clathrin-mediated endocytosis (He et al., 2015; He et al., 2017; He et al., 2019).

XL $\alpha$ s expression has been shown to occur exclusively from the paternal allele (Hayward et al., 1998), unlike G $\alpha$ , which is biallelic in most tissues. Thus, a *GNAS* mutation is predicted to affect XL $\alpha$ s only if it resides on the paternal allele. For example, the *GNAS* mutations causing pseudohypoparathyroidism type-1a are inherited maternally (Davies and Hughes, 1993) and, therefore, disrupt one copy of G $\alpha$  without affecting XL $\alpha$ s. In contrast, the same mutations in patients with pseudo-pseudohypoparathyroidism are inherited paternally and thus disrupt both XL $\alpha$ s and one copy of G $\alpha$ . The severe intrauterine growth retardation observed in pseudo-pseudohypoparathyroidism is attributed to XL $\alpha$ s deficiency (Richard et al., 2013). In addition, recent studies have described patients with maternal uniparental disomy of chromosome 20 (matUPD20, MIM: 617352)—the genomic region comprising *GNAS*—who display Silver-Russell syndrome-like features including perinatal growth retardation and intractable feeding difficulties (Mulchandani et al., 2016; Kawashima et al., 2018). The phenotypes associated with matUPD20 are similar to those observed in children with large paternal *GNAS* deletions (Aldred et al., 2002; Genevieve et al., 2005) and thus attributed largely to XL $\alpha$ s deficiency. Moreover, a recent study described an adult patient with hypophosphatemia and osteopetrosis who carried a nonsense mutation within the first XL $\alpha$ s exon (Chen et al., 2020). This defect was also paternally inherited, consistent with the evidence that XL $\alpha$ s is expressed from the paternal allele. Nevertheless, a study demonstrated XL $\alpha$ s expression from both alleles in human bone marrow stromal cells (BMSCs) from normal and fibrous dysplastic tissues (Michienzi et al., 2007). The analyzed BMSCs were clonogenic, and interestingly, G $\alpha$  expression was also shown to be allelically, but randomly, skewed, suggesting that the observed alterations in allelic XL $\alpha$ s and G $\alpha$  expression may have been secondary to the cloning.

BMSCs include mesenchymal progenitor/stem cells capable of differentiating into multiple different lineages. G $\alpha$  signaling promotes the commitment of mesenchymal progenitors into the osteoblast lineage while restricting osteoblast differentiation (Wu et al., 2011). Accordingly, a gain-of-function *GNAS* mutation results in the aberrant differentiation of BMSCs into osteoblasts, the primary cellular mechanism underlying fibrous dysplasia of bone (Xiao et al., 2019). The causative *GNAS* mutations are heterozygous and located in exons shared by G $\alpha$  and XL $\alpha$ s (Weinstein et al., 1991; Schwindinger et al., 1992). It has been shown that these mutations increase the baseline activity of not only G $\alpha$  but also XL $\alpha$ s (Klemke et al., 2000; He et al., 2015). Thus, whether XL $\alpha$ s is expressed monoallelically or biallelically in BMSCs could have strong implications for fibrous dysplasia pathogenesis. Moreover, as mentioned above, the phenotypes attributed to the loss of XL $\alpha$ s *in vivo* are based on the notion that XL $\alpha$ s is expressed in an exclusively paternal manner. If, however, tissue-specific biallelic XL $\alpha$ s expression exists, then our understanding of its physiological roles and its involvement in *GNAS*-related diseases may have to be revised.

In this study, we investigated the allele-specific expression of XL $\alpha$ s in non-clonal mouse and human BMSCs and other cells and tissues. We quantitated allelic contribution by employing next-generation sequencing (NGS) of RT-PCR amplicons carrying a polymorphism. Our results revealed a significant contribution from the maternal *GNAS* allele in non-differentiated BMSCs but not in osteogenically differentiated BMSCs or calvarial osteoblasts.

## MATERIALS AND METHODS

### Mice

XL $\alpha$ s knockout (XLKO) mice, carrying a disruption in the first exon of XL $\alpha$ s, have been described (Plagge et al., 2004) and maintained in the CD1 background. Wildtype 129/Sv and C57BL/6 mice (Jackson Laboratory) were mated to obtain F1 generation hybrid offspring. Both male and female mice were analyzed. All mice experiments were conducted according to the accepted standards of the Institutional Animal Care and Use Committee and approved by the Massachusetts General Hospital Subcommittee on Research Animal Care.

### Restriction Digestion for Confirming Maternal and Paternal XLKO Samples and Determining the Parental Contribution of *Gnas* Transcripts

The methylation-sensitive restriction enzyme *HpaII* (New England Biolabs) was used to digest the genomic DNA (1  $\mu$ g) from tails of offspring derived from matings between heterozygous XLKO mice. Digested DNA was purified using the QIAquick PCR purification kit (Qiagen) and eluted with 30  $\mu$ l water. Then, 2  $\mu$ l of each sample was used as a template for genotyping PCR, as described (Plagge et al., 2004). To determine the parental contribution of G $\alpha$ , XL $\alpha$ s, and A/B transcripts,

RT-PCR products from tissues of mice heterozygous for the C-to-G SNP in exon 11 (rs13460569) were incubated (37°C, 6 h) with *Ban*II (New England BioLabs) and analyzed by agarose gel electrophoresis, as described (Tafaj et al., 2017).

## Mouse Primary Cell Cultures and Osteogenic Differentiation

Mouse BMSCs were harvested by flushing the marrow out of long bones (femurs and tibias) of 14 week-old mice, as described (Wu et al., 2011). Cells were plated at a density of  $0.5 \times 10^6$  to  $1 \times 10^6$  cells/cm<sup>2</sup> and cultured in Dulbecco's Modified Eagle's Medium (DMEM) (Gibco, United States) containing 10% Fetal Bovine Serum (FBS) (Hyclone, United States). Non-adherent cells were washed off, and the adherent cells were cultured for 1 week, followed by RNA extraction. Primary calvarial pre-osteoblasts were isolated at postnatal day five by serial collagenase digestion, as described (Mariot et al., 2011). Cells were seeded at a density of 10,000 cells/well in 12-well plates and cultured in Modified Eagle's Medium (MEM) (Gibco, United States) containing 10% FBS. Osteoblastic differentiation was induced by adding ascorbic acid (50  $\mu$ g/ml) and  $\beta$ -glycerol phosphate (10 mM) (Sigma-Aldrich), as described (Wu et al., 2011). Differentiation medium for BMSCs also included 10 nM dexamethasone (Sigma-Aldrich).

## Human BMSCs

Cells were obtained from participants who underwent total hip arthroplasty surgery at Boston Medical Center between 2019 and 2020. All human research was done under a Boston University School of Medicine Institutional Research Board Approved protocol: "Bone Tissues Repository," IRB Number: H-35199, with patients' consents per current HIPAA regulations prior to surgery and specimen collection. The femoral head and reamings, from the coring of the acetabulum, were collected during total hip arthroplasty. After multiple washes using DPBS (Hyclone Laboratories) containing an antibiotic-antimycotic mixture (Thermo Fischer Scientific) cells were suspended in DPBS. 24 million cells/well were seeded in each well of 6-well plates (Corning Inc.), treated with Animal Component-Free Cell Attachment Substrate (Stem Cell Technologies) diluted 1:150 in DPBS. Cells were cultured in an incubator at 37°C, 5% CO<sub>2</sub>, and > 90% humidity. A half media change was performed on day 4 and a full media change on day six after plating. Cells were then grown in basal medium supplemented with osteoinductive factors (Stem Cell Technologies) for 21 days before RNA extraction.

## Total RNA Extraction, RT-PCR and qRT-PCR Amplification

Total RNA of mouse organs was extracted by using Trizol<sup>®</sup> Reagent (Life Technologies) followed by the Qiagen RNeasy<sup>®</sup> Plus Mini Kit. Total RNA of human BMSCs was extracted using 4 M Guanidine-HCl, 1% Triton X-100, 10 mM Tris HCl, 2 mM EDTA (pH 7.4). cDNA was synthesized using the New England Biolabs ProtoScript II First-strand cDNA synthesis kit.

Total RNA of calvarial osteoblasts and BMSC were isolated by using the Qiagen RNeasy<sup>®</sup> Plus Mini kit. One  $\mu$ g total RNA

was reverse transcribed using the Superscript III First-Strand Synthesis System (Invitrogen) and then subjected to PCR using the PCR Master Mix (Promega). PCR mixture contained 2  $\mu$ L cDNA in a final volume of 20  $\mu$ L. PCR included 1 cycle at 94°C for 5 min, followed by 40 cycles of 94°C for 30 s, 56°C for 30 s and 72°C for 2 min, and a final extension at 72°C for 7 min. For XL $\alpha$ s and A/B, nested PCR was performed using, as template, the primary PCR product diluted 1:10 or 1:2, respectively. qRT-PCR included 1 cycle at 50°C for 2 min and 94°C for 15 min, followed by 50 cycles of 94°C for 15 s, 60°C for 20 s, and 72°C for 20 s. The PCR primers are listed in **Supplementary Table 1**.

## Sequence Analysis of RT-PCR Products

The RT-PCR products were purified by the QIAquick PCR Purification kit. Both Sanger sequencing and NGS was performed at the Massachusetts General Hospital DNA Core. Primers for Sanger sequencing were the same as PCR primers. For NGS, purified PCR products were first fragmented and then subjected to NGS library preparation, followed by sequencing on the Illumina MiSeq. The reads were analyzed following automated *de novo* sequence assembly. The authenticity of the amplicons was confirmed by the unique first exon sequences of XL $\alpha$ s and A/B. To determine the relative contributions of the parental alleles, the ratio of reads containing one of the nucleotides to the total number of reads at rs13460569 (mouse) or rs7121 (human) was calculated for each sample.

## Genomic DNA Methylation Analysis

Genomic DNA (600 ng) from non-differentiated and differentiated BMSCs (the same samples as those used for allelic XL $\alpha$ s expression) was treated with sodium bisulfite by using the EZ DNA Methylation gold kit (Zymo Research), and the converted DNA was recovered in 10  $\mu$ L. Primary PCR was performed using 2  $\mu$ L bisulfite-treated DNA as template in a total reaction volume of 40  $\mu$ L. The nested PCR used 2  $\mu$ L of the primary PCR product. PCR included initial denaturation at 95°C for 5 min, 35 cycles of 95°C for 30 s, 56°C for 30 s, 72°C for 30 s, and final extension at 72°C for 10 min. Primers for the region within XL $\alpha$ s exon were previously described (Liu et al., 2000). Primers for the XL $\alpha$ s promoter were as follows: 5'-GATGGGGAGGGAGGTTTTTA-3' (forward) and 5'-AAACTAAAACCCAAAACCATAACT-3' (reverse). Nested PCR used the same forward primer together with the following reverse primer: 5'-TCACCTTCTAATTACACTTACCC-3'. The amplicons were subjected to NGS at the Massachusetts General Hospital DNA Core. To calculate the degree of methylation, paired-end NGS reads were aligned using the BWA-MEM algorithm to a reference reflecting bisulfite-induced alterations except for the CpG dinucleotides. The FreeBayes variant detector was then used to identify each C-to-T variant and the allelic balance (i.e., C is methylated and T non-methylated). BWA-MEM and FreeBayes were run on the Galaxy platform<sup>1</sup> (Afgan et al., 2018).

<sup>1</sup><https://usegalaxy.org/>

## Statistical Analyses

Outliers were identified by the Grubbs test and excluded. One-way ANOVA followed by Tukey's *post-hoc* test was used to analyze the differences among three or more groups. The student's *t*-test (two-tailed) was used between two groups. The paired Student's *t*-test (two-tailed) was employed for the differences between non-differentiated and differentiated BMSC samples. Wilcoxon rank-sum test was performed to compare the groups regarding the distribution of the data. One-sample *t*-test was performed to determine the significance of the difference between the maternal expression in non-differentiated BMSCs and the hypothetical value of 0%.  $P < 0.05$  were considered significant. Analyses were performed using Prism 8 (GraphPad).

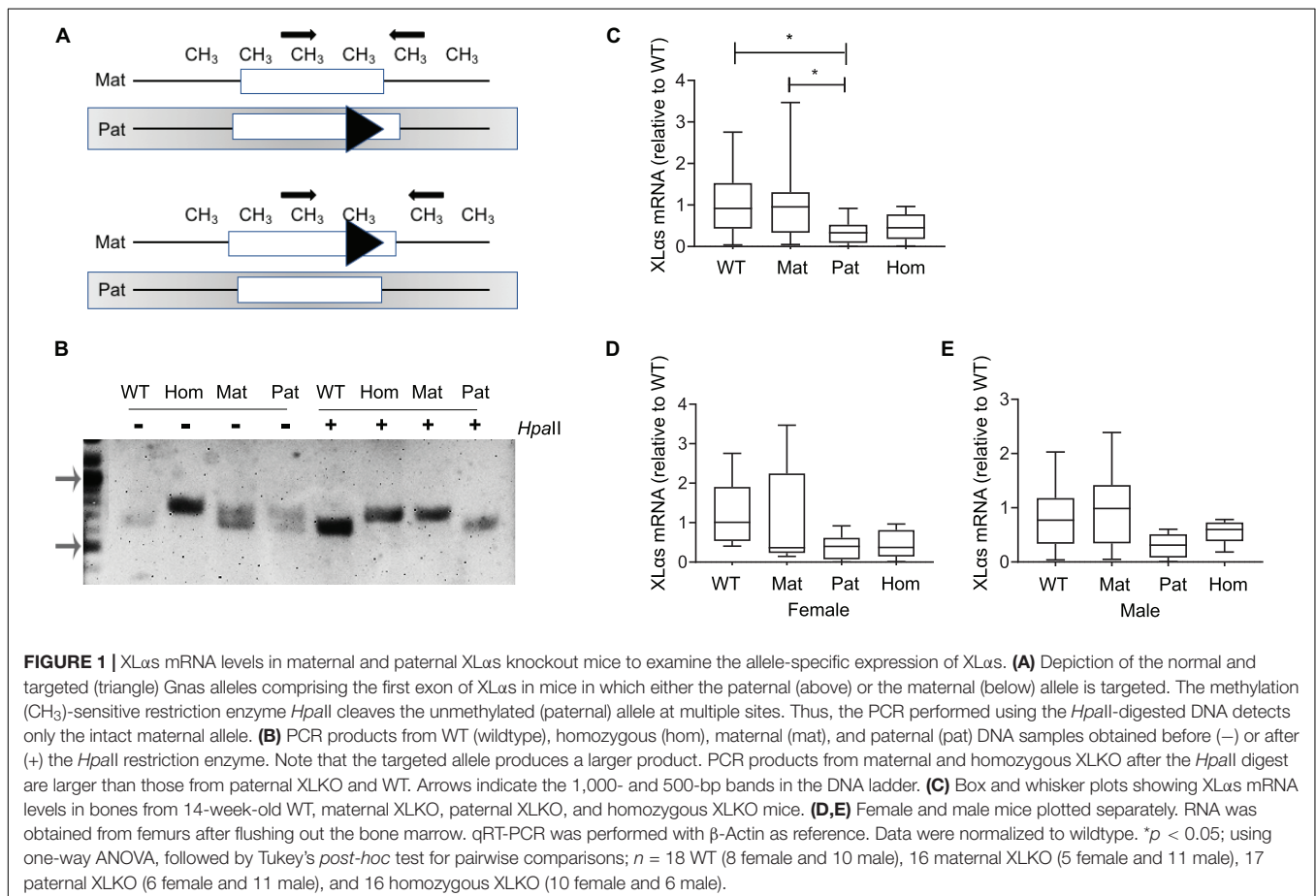
## RESULTS

### Comparing XL $\alpha$ s mRNA Levels in Wildtype and XLKO Mice to Determine Allele-Specific XL $\alpha$ s Expression

To examine the allelic expression profile of XL $\alpha$ s in bone, we first employed adult XLKO mice, because disruption of paternal XL $\alpha$ s first exon in those mice was reported to cause a dramatic reduction of XL $\alpha$ s transcript levels in various tissues

(Plagge et al., 2004). The maternal, paternal, and homozygous XLKO mice were derived from matings between heterozygous XLKO mice. The previously described genotyping approach for these mice (Plagge et al., 2004) is unable to distinguish maternal from paternal XLKO mice. We thus performed genotyping before and after digestion of genomic DNA with the methylation-sensitive restriction enzyme *HpaII*, which cleaves the unmethylated, paternal allele at multiple sites and, thereby, prevents it from serving as a template in PCR (Figure 1A). The PCR performed following the *HpaII* digest detected only the intact maternal allele and allowed us to identify the parental origin of the targeted allele. In the absence of the *HpaII* digestion, heterozygotes showed a double band, the upper one representing the targeted allele, and wildtype (WT) and homozygous XLKO mice yielded only the smaller or the larger product, respectively (Figure 1B). Following the *HpaII* digest, only the smaller PCR product was detected in WT and paternal XLKO mice, and only the larger PCR product was observed in homozygous and maternal XLKO mice (Figure 1B).

qRT-PCR using total RNA from femur samples (bone marrow flushed out) showed that XL $\alpha$ s mRNA levels were significantly lower in paternal XLKO mice than in WT or maternal XLKO littermates (Figure 1C). While this finding was consistent with the silencing of the maternal allele in bone, other comparisons did not corroborate this conclusion. No statistically significant



differences could be detected between the levels in homozygous XLKO mice and either WT or maternal XLKO (**Figure 1C**). Separate analysis of males and females did not reveal any significant differences between the groups, owing partly to the reduced sample sizes (**Figures 1D,E**).

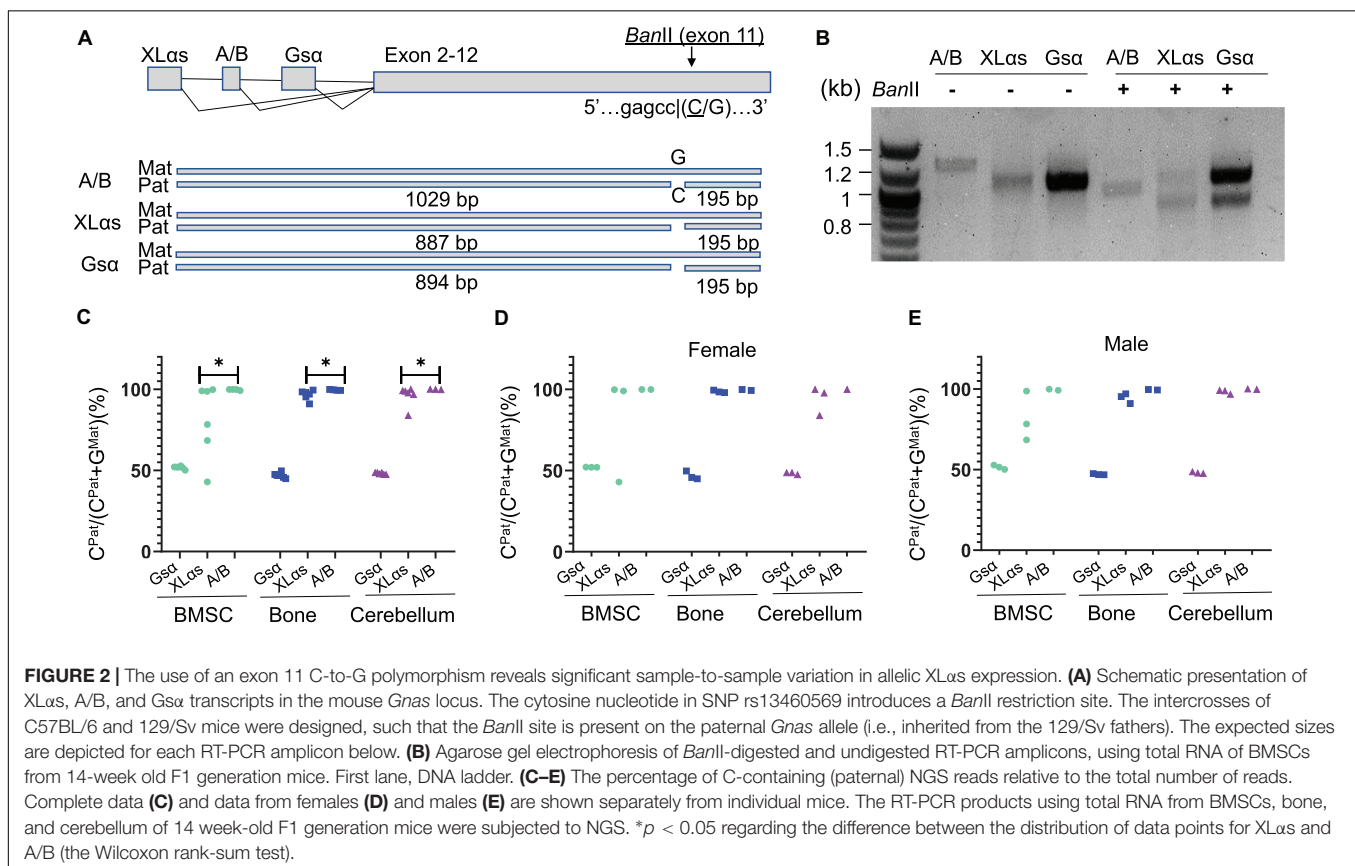
## Intercrosses of C57BL/6 and 129/Sv Mice Allows Identification of Parental *Gnas* Alleles

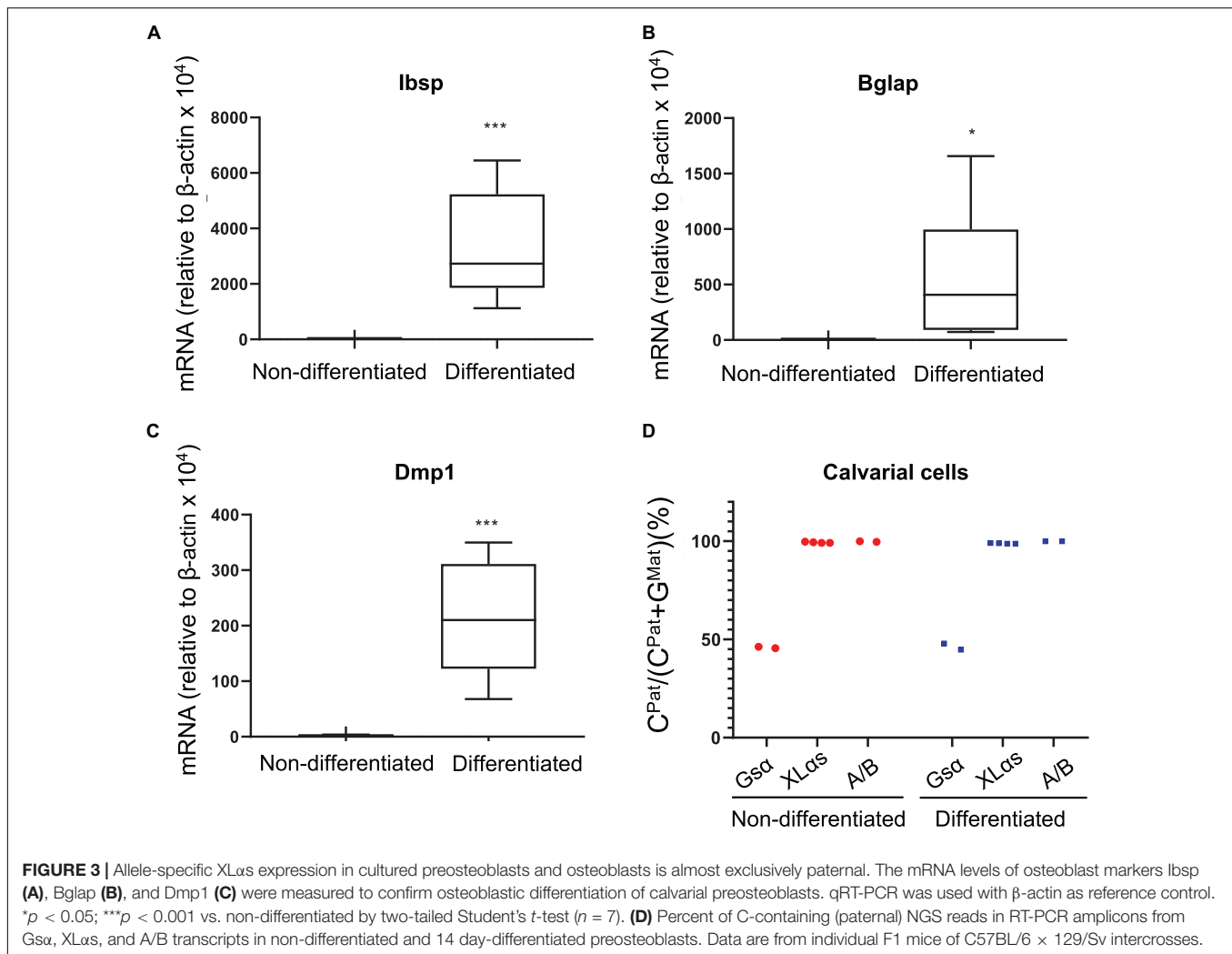
To determine allelic XL $\alpha$ s expression without relying on gene disruption, we then took advantage of a polymorphism located in *Gnas* exon 11, as described (Tafaj et al., 2017). The 129/Sv mice carry a cytosine (C), while C57BL/6 and CD1 strains carry a guanine (G) in the G $\alpha$  transcript (NM\_201616.2, c.1009; rs13460569). We thus set up matings between 129/Sv males and C57BL/6 females and analyzed the offspring at age 14 weeks. RT-PCR using total RNA isolated from BMSCs amplified specific products from G $\alpha$ , XL $\alpha$ s, and A/B transcripts including the exon 11 polymorphism, and those products were then digested with *Ban*II, a restriction enzyme that recognizes the polymorphism and differentially cleaves the paternally-derived C-containing products (**Figure 2A**). *Ban*II partially cleaved the G $\alpha$ -derived products (**Figure 2B**), consistent with the previously demonstrated biallelic expression of this *Gnas* product in multiple tissues (Tafaj et al., 2017). In contrast, the A/B-derived products were completely cleaved, indicating that, consistent

with previous observations (Tafaj et al., 2017), the A/B expression was nearly completely paternal (**Figure 2B**). A significant portion of the XL $\alpha$ s-derived RT-PCR products was cleaved; however, a faint band representing non-cleaved products were also visible, suggesting that XL $\alpha$ s expression may not be exclusively paternal in BMSCs (**Figure 2B**).

## NGS to Quantitate the Parental Origin of XL $\alpha$ s Expression

To have a quantitative assessment of XL $\alpha$ s expression from paternal vs. maternal *Gnas* alleles, we then subjected the RT-PCR products to NGS. Providing sequence data from thousands of molecules from each PCR amplicon, this approach revealed the origin of each read with respect to its parental origin, i.e., C-containing reads are derived from the paternal allele, while G-containing reads are from the maternal allele. We analyzed BMSCs and femur, as well as cerebellum, in which XL $\alpha$ s was shown to be expressed at high levels (Pasolli et al., 2000). As shown in **Figures 2C–E** and **Supplementary Table 2**, the G $\alpha$  products contained ~50% C-containing products in all the tissues tested, thus confirming the biallelic transcription of G $\alpha$ . The C-containing reads in A/B transcript-derived PCR products were nearly 100% of the total in all three tissues, indicating exclusive paternal expression. In XL $\alpha$ s-derived RT-PCR products, however, the ratio of C-containing to G-containing reads varied significantly from sample to sample, particularly in BMSCs,





ranging from 43.0 to 99.9% among six independent samples (Figures 2C–E and Supplementary Table 2). Modest sample-to-sample variation was also detectable in bone (83.7–99.6%) and cerebellum (83.8–100%; Figures 2C–E and Supplementary Table 2), and the variation observed in XL $\alpha$ s-derived products was significantly different from the variation observed in A/B-derived products in all three tissues.

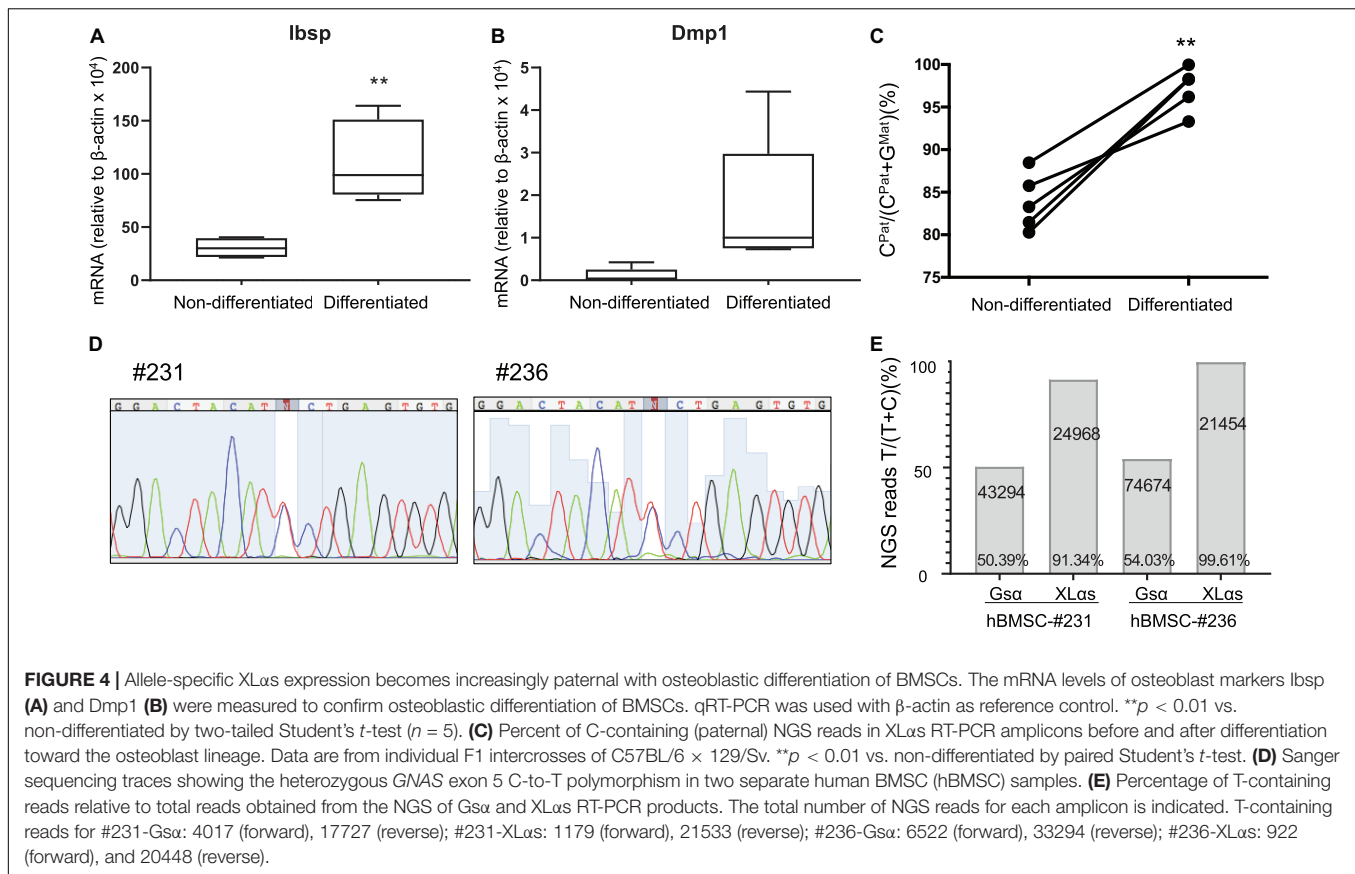
### Allelic XL $\alpha$ s Expression in Differentiated Osteoblasts

As another type of cultured primary cells, we examined mouse calvarial pre-osteoblasts from the C57BL/6-129/Sv intercrosses before and after culturing them under osteogenic conditions for 14 days. qRT-PCR experiments confirmed the osteoblast markers bone sialoprotein (Ibsp), osteocalcin (Bglap), and dentin matrix protein-1 (Dmp1) (Figures 3A–C). The NGS analysis of G $\alpha$ -derived RT-PCR products showed comparable numbers of C- and G-containing reads in both non-differentiated and differentiated cells, indicating biallelic expression (Figure 3D). In contrast, C-containing reads were nearly 100% of total reads for both XL $\alpha$ s

and A/B products in those cells and there was no evidence of variation in the allelic XL $\alpha$ s expression (Figure 3D).

We then analyzed a new set of BMSCs both before and after osteogenic differentiation, which was confirmed by measuring the levels of Ibsp and Dmp1 mRNA (Figures 4A,B). In this new set of samples, while the paternal expression of A/B was nearly 100%, the paternal XL $\alpha$ s expression varied modestly from 80.3 to 88.5% of total (Figure 4C and Supplementary Table 3). This finding confirmed the significant contribution from the maternal allele to XL $\alpha$ s expression (mean =  $16.1 \pm 1.5\%$ ,  $p < 0.001$  vs. the hypothetical 0% maternal). Combined, the mean maternal expression in all our BMSC samples ( $n = 11$ ) was  $17.6 \pm 4.9\%$  (95% confidence interval: 6.6–28.6%;  $p < 0.01$  vs. the hypothetical value of 0%). Strikingly, when cells were grown under osteoinductive conditions for 2 weeks, the expression of XL $\alpha$ s shifted in the favor of the paternal allele, from  $83.9 \pm 1.5\%$  paternal in non-differentiated to  $97.2 \pm 1.1\%$  paternal in differentiated BMSCs (Figure 4C).

We also tested human BMSCs from two unrelated individuals, employing a C-to-T polymorphism located in GNAS exon 5 (rs7121, chr20:58903752, hg38). The samples (#231 and #236)



were cultured under osteogenic conditions before examining the relative contribution of each allele to *Gsa* and XL $\alpha$ s expression. Sanger sequencing of *Gsa*-derived RT-PCR products revealed that both samples were heterozygous for the polymorphism (**Figure 4D**). Subsequent NGS of those products showed comparable numbers of reads containing either C or T at the polymorphic site, with T-containing reads making up 50.4 or 54.0% of total reads (**Figure 4E**). In contrast, NGS of XL $\alpha$ s-derived RT-PCR products yielded 91.3 and 99.6% T-containing reads in #231 and #236, respectively (**Figure 4E**), indicating predominantly or nearly exclusively monoallelic expression.

### Differential DNA Methylation at the Genomic XL $\alpha$ s Locus

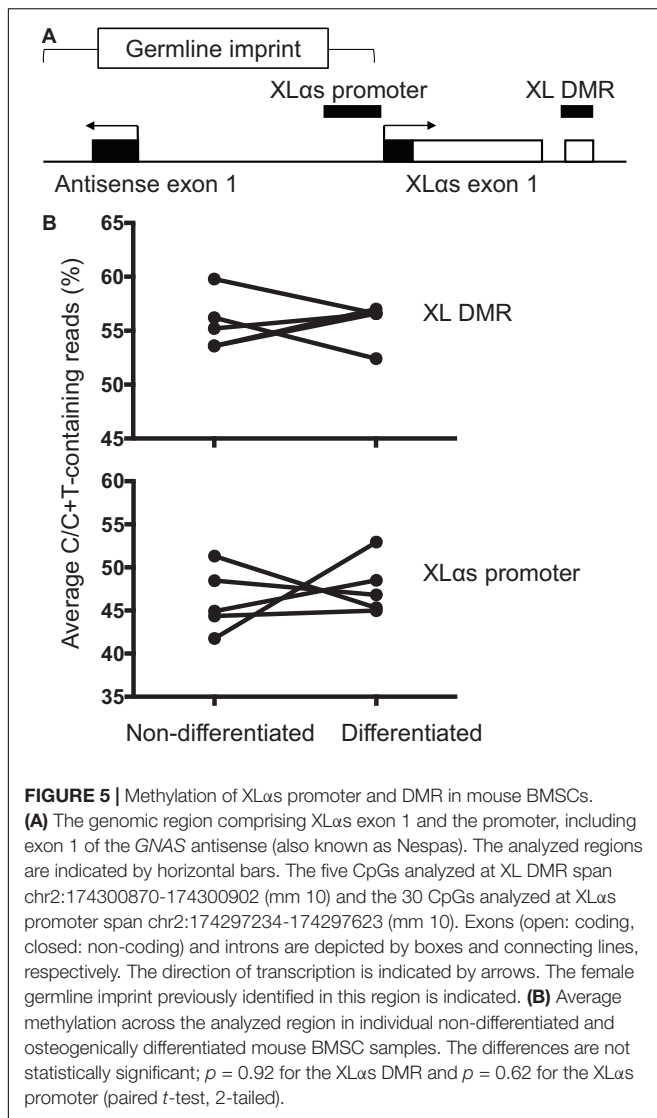
The genomic region comprising the first XL $\alpha$ s exon is differentially methylated, consistent with the monoallelic expression of XL $\alpha$ s transcripts. We thus analyzed the degree of methylation in the previously described region (Liu et al., 2000). PCR amplicons derived from bisulfite-treated genomic DNA were subjected to NGS, thus allowing accurate relative quantification of unmethylated (converted to T) and methylated (protected) CpGs at multiple sites. The results, however, showed no significant differences in the overall degree of methylation between non-differentiated and differentiated BMSCs (average of 55.7 and 55.8% of total, respectively; **Figures 5A,B**). We also analyzed the methylation status of a second region,

which overlaps the XL $\alpha$ s promoter (Williamson et al., 2006; Aydin et al., 2009; **Figure 5A**). The methylation of individual CpGs and the average methylation across the amplicon were comparable between non-differentiated and differentiated BMSCs (average 46.2 and 47.7%, respectively; **Figure 5B** and **Supplementary Table 4**).

## DISCUSSION

In this study, we examined the parental contribution of *GNAS* allele to XL $\alpha$ s expression in non-clonal BMSCs and other murine tissues. In bone and cultured calvarial osteoblasts, XL $\alpha$ s expression was nearly exclusively paternal. In contrast, substantial maternal contribution was detected in non-differentiated BMSCs. The expression of *Gsa* was biallelic and that of A/B was virtually exclusively paternal in all the investigated cells/tissues.

To assess allelic XL $\alpha$ s expression, we first measured XL $\alpha$ s mRNA levels in paternal, maternal, and homozygous XLKO mice and their wildtype littermates. A similar approach has been used to measure the monoallelic expression of *Gsa* in certain tissues, such as proximal renal tubules (Turan et al., 2014). However, although the results appeared broadly consistent with an allelic bias of XL $\alpha$ s expression in bone, the mRNA levels varied widely, even within the same genotype. As this approach relied on the loss of XL $\alpha$ s production from the disrupted allele, this variability



may reflect some detectable levels of XL $\alpha$ s mRNA being made from the latter allele, in addition to the outbred CD1 background in which XLKO mice had to be maintained (Plagge et al., 2004).

As an alternative approach, we utilized a known polymorphism in the mouse *Gnas* locus. We subjected the RT-PCR products to NGS, since it has been utilized for quantitatively detecting mosaic single nucleotide variants in clinical settings (Narumi et al., 2013). Indeed, NGS allowed us to obtain sequence information from thousands of reads and distinguish the allelic origin of the products. We analyzed the allele-specific XL $\alpha$ s and G $\alpha$ s expression in human BMSCs similarly, using NGS and a common polymorphism (Campbell et al., 1994). In the human samples, genotypes of the donors' parents were unknown. Therefore, although we could quantify the allele-specific expression, we were unable to determine the parental origin.

Michienzi et al. examined clonal BMSCs from wildtype and fibrous dysplasia-derived samples and showed evidence of

biallelic XL $\alpha$ s expression, as well as parental G $\alpha$ s expression that appeared asymmetrical (Michienzi et al., 2007). We analyzed non-clonal BMSCs passed no more than three times. In total, we found biallelic XL $\alpha$ s expression in one sample and substantial deviation from monoallelic expression in seven samples, while the results from the remaining three samples were consistent with nearly exclusive paternal expression. There might be an influence of cell culture on our results. Nonetheless, no such variation was observed among our calvarial osteoblast samples, which were also cultured. Moreover, in BMSCs that were differentiated in culture toward the osteoblast lineage, the XL $\alpha$ s expression became more significantly paternal, arguing against the possibility that culture conditions caused a relaxation of XL $\alpha$ s imprinting.

A plausible explanation for the observed variation in allelic XL $\alpha$ s expression in our BMSC samples may be cellular heterogeneity, as BMSCs are known to be heterogeneous with variable representations of cell types in different samples (Kfoury and Scadden, 2015). Therefore, it is likely that XL $\alpha$ s is expressed biallelically in a certain subset of cells in the bone marrow, as well as in some other tissues. Regarding the study by Michienzi et al. (2007), the analyzed clonogenic BMSCs may have been derived from the cell-type(s) in which XL $\alpha$ s expression is biallelic. Alternatively, the maternal XL $\alpha$ s promoter may be active in all cell types in the BMSC samples but at a lower level than the paternal XL $\alpha$ s promoter. However, when considering the heterogeneity of BMSCs regarding cell types and the variation we observed among the samples, the former possibility appears more plausible. The finding that substantial XL $\alpha$ s expression occurs from the maternal allele in certain cell types has important implications. The physiological roles of XL $\alpha$ s *in vivo* have thus far been deduced from findings in mice or patients in whom the paternal XL $\alpha$ s allele is disrupted alone, assuming a complete loss of this protein in all tissues. According to our results, some of those interpretations could be at least partially incorrect.

We found paternal XL $\alpha$ s expression in mouse whole bones, although significant but modest sample-to-sample variation was observed in the parental contribution, as opposed to A/B expression, which appeared consistently  $\sim 100\%$  paternal. XL $\alpha$ s is substantially expressed in the cerebellum (Pasolli et al., 2000). We also detected mild variation in the allelic expression of XL $\alpha$ s among our mouse cerebellum samples, suggesting that in both bone and cerebellum, there may be a small subset of cells in which XL $\alpha$ s expression is biallelic.

Unlike the allelic expression data, we did not detect differences in DNA methylation between non-differentiated and differentiated BMSCs. The data for the methylation analysis reflected all the cells in the sample while the expression data originated only from cells that express XL $\alpha$ s. Since the methylation differences are expected to occur only in XL $\alpha$ s-expressing cells, they may have remained under our detection limit, particularly if those cells are scarce. Alternatively, other methylated regions or regulatory events may dictate the allelic shift of XL $\alpha$ s expression during osteogenic differentiation. The analyzed XL $\alpha$ s promoter region lies within a germline imprint including the *Gnas* antisense exon 1 (also known as *Nespas*; Coombes et al., 2003; see Figure 5A). It is possible that a different part of this germline imprint regulates the XL $\alpha$ s promoter

activity. Also, a methylation-independent mechanism may be involved, considering that an “uncoupling” of allelic silencing and promoter DNA methylation has been described for the Nespas-mediated regulation of the Nesp55 promoter activity (Williamson et al., 2011). The regulation of allelic expression in this locus is certainly complex. It is also worth mentioning that the analyzed XL $\alpha$ s promoter region is orthologous to human GNAS-AS2, a region shown to be severely hypomethylated (i.e., loss of methylation) in patients with both sporadic and familial pseudohypoparathyroidism type-Ib (MIM: 603233) (Rochtus et al., 2016). Whether the hypomethylation is associated with biallelic XL $\alpha$ s expression is unknown.

Tissue- or cell type-specificity has been shown for the monoallelic expression of some transcripts, including Gs $\alpha$ , which is biallelic in most but predominantly maternal in some tissues (Yu et al., 1998). Conversely, Dlk1, a product of the imprinted gene cluster on chromosome 14, is paternally expressed nearly in all tissues but exhibits biallelic expression in postnatal neural stem cells and niche astrocytes (Ferron et al., 2011). Our observations regarding the allelic expression of XL $\alpha$ s are analogous to those documented for Dlk1 and supports the likelihood that XL $\alpha$ s is expressed biallelically in certain cell types. Identification of those cells may reveal important novel roles of XL $\alpha$ s.

In summary, our findings indicate that the maternal GNAS allele contributes significantly to XL $\alpha$ s expression in BMSCs. Thus, altered XL $\alpha$ s actions could be involved in at least some of the phenotypes associated with GNAS mutations even if the mutation is maternal.

## DATA AVAILABILITY STATEMENT

The original contributions presented in the study are included in the article/**Supplementary Material**, further inquiries can be directed to the corresponding author/s.

## ETHICS STATEMENT

The studies involving human participants were reviewed and approved by the Boston University School of Medicine Institutional Research Board. The patients/participants provided their written informed consent to participate in this study. The animal study was reviewed and approved by Subcommittee

on Research Animal Care, Massachusetts General Hospital. Written informed consent was obtained from the owners for the participation of their animals in this study.

## AUTHOR CONTRIBUTIONS

QC: investigation, methodology, formal analysis, visualization, writing, and original draft. CA, BA, CR, MG, and MD: investigation. AP and LG: resources, writing—review, and editing. QH: investigation, methodology, writing—review, and editing. MB: conceptualization, formal analysis, funding acquisition, supervision, visualization, writing—original draft. All authors contributed to the article and approved the submitted version.

## FUNDING

This work was funded in part by a research grant from the United States. National Institutes of Health/National Institute of Diabetes and Digestive and Kidney Diseases (R01DK073911 to MB). The statistical analyses were conducted with support from Harvard Catalyst | The Harvard Clinical and Translational Science Center (National Center for Advancing Translational Sciences, National Institutes of Health Award UL1TR002541) and financial contributions from Harvard University and its affiliated academic healthcare centers. The content is solely the responsibility of the authors and does not necessarily represent the official views of Harvard Catalyst, Harvard University and its affiliated academic healthcare centers, or the National Institutes of Health.

## ACKNOWLEDGMENTS

We thank Gavin Kelsey (Babraham Institute, Cambridge, United Kingdom) for kindly providing the XLKO mice.

## SUPPLEMENTARY MATERIAL

The Supplementary Material for this article can be found online at: <https://www.frontiersin.org/articles/10.3389/fgene.2021.680537/full#supplementary-material>

## REFERENCES

- Afgan, E., Baker, D., Batut, B., van den Beek, M., Bouvier, D., Cech, M., et al. (2018). The Galaxy platform for accessible, reproducible and collaborative biomedical analyses: 2018 update. *Nucleic Acids Res.* 46, W537–W544.
- Aldred, M. A., Aftimos, S., Hall, C., Waters, K. S., Thakker, R. V., Trembath, R. C., et al. (2002). Constitutional deletion of chromosome 20q in two patients affected with albright hereditary osteodystrophy. *Am. J. Med. Genet.* 113, 167–172. doi: 10.1002/ajmg.10751
- Aydin, C., Aytan, N., Mahon, M. J., Tawfeek, H. A., Kowall, N. W., Dedeoglu, A., et al. (2009). Extralarge XL $\alpha$ s (XXL $\alpha$ s), a variant of stimulatory G protein alpha-subunit (Gs $\alpha$ ), is a distinct, membrane-anchored GNAS product that can mimic Gs $\alpha$ . *Endocrinology* 150, 3567–3575. doi: 10.1210/en.2009-0318
- Bastepe, M. (2007). The GNAS locus: quintessential complex gene encoding g $\alpha$ lpha, XL $\alpha$ s, and other imprinted transcripts. *Curr. Genomics* 8, 398–414. doi: 10.2174/138920207783406488
- Bastepe, M., Gunes, Y., Perez-Villamil, B., Hunzelman, J., Weinstein, L. S., and Jüppner, H. (2002). Receptor-mediated adenylyl cyclase activation through XL $\alpha$ s, the extra-large variant of the stimulatory G Protein alpha-Subunit. *Mol. Endocrinol.* 16, 1912–1919. doi: 10.1210/me.2002-0054
- Campbell, R., Gosden, C. M., and Bonthron, D. T. (1994). Parental origin of transcription from the human GNAS1 gene. *J. Med. Genet.* 31, 607–614. doi: 10.1136/jmg.31.8.607
- Chen, X., Meng, Y., Tang, M., Wang, Y., Xie, Y., Wan, S., et al. (2020). A paternally inherited non-sense variant c.424G>T (p.G142\*) in the first exon of XL $\alpha$ s in an adult patient with hypophosphatemia and osteopetrosis. *Clin. Genet.* 97, 712–722. doi: 10.1111/cge.13734

- Coombes, C., Arnaud, P., Gordon, E., Dean, W., Coar, E. A., Williamson, C. M., et al. (2003). Epigenetic properties and identification of an imprint mark in the Nesp-Gnasxl domain of the mouse Gnas imprinted locus. *Mol. Cell Biol.* 23, 5475–5488. doi: 10.1128/mcb.23.16.5475-5488.2003
- Davies, A. J., and Hughes, H. E. (1993). Imprinting in Albright's hereditary osteodystrophy. *J. Med. Genet.* 30, 101–103.
- Ferron, S. R., Charalambous, M., Radford, E., McEwen, K., Wildner, H., Hind, E., et al. (2011). Postnatal loss of Dlk1 imprinting in stem cells and niche astrocytes regulates neurogenesis. *Nature* 475, 381–385. doi: 10.1038/nature10229
- Genevieve, D., Sanlaville, D., Faivre, L., Kottler, M. L., Jambou, M., Gosset, P., et al. (2005). Paternal deletion of the GNAS imprinted locus (including Gnasxl) in two girls presenting with severe pre- and post-natal growth retardation and intractable feeding difficulties. *Eur. J. Hum. Genet.* 13, 1033–1039. doi: 10.1038/sj.ejhg.5201448
- Hayward, B., Kamiya, M., Strain, L., Moran, V., Campbell, R., Hayashizaki, Y., et al. (1998). The human GNAS1 gene is imprinted and encodes distinct paternally and biallelically expressed G proteins. *Proc. Natl. Acad. Sci. U.S.A.* 95, 10038–10043. doi: 10.1073/pnas.95.17.10038
- He, Q., Bouley, R., Liu, Z., Wein, M. N., Zhu, Y., Spatz, J. M., et al. (2017). The large G protein alpha-subunit XL $\alpha$ s limits clathrin-mediated endocytosis and regulates tissue iron levels in vivo. *Proc. Natl. Acad. Sci. U.S.A.* 114, E9559–E9568.
- He, Q., Shumate, L. T., Matthias, J., Aydin, C., Wein, M. N., Spatz, J. M., et al. (2019). A G protein-coupled, IP3/protein kinase C pathway controlling the synthesis of phosphaturic hormone FGF23. *JCI Insight* 4:e125007.
- He, Q., Zhu, Y., Corbin, B. A., Plagge, A., and Bastepe, M. (2015). The G protein alpha subunit variant XL $\alpha$ phas promotes inositol 1,4,5-trisphosphate signaling and mediates the renal actions of parathyroid hormone in vivo. *Sci. Signal.* 8:ra84. doi: 10.1126/scisignal.aaa9953
- Kawashima, S., Nakamura, A., Inoue, T., Matsubara, K., Horikawa, R., Wakui, K., et al. (2018). Maternal uniparental disomy for chromosome 20: physical and endocrinological characteristics of five patients. *J. Clin. Endocrinol. Metab.* 103, 2083–2088.
- Kehlenbach, R. H., Matthey, J., and Huttner, W. B. (1994). XL $\alpha$ s is a new type of G protein (Erratum in Nature 1995 375:253). *Nature* 372, 804–809.
- Kelsey, G. (2010). Imprinting on chromosome 20: tissue-specific imprinting and imprinting mutations in the GNAS locus. *Am. J. Med. Genet. C Semin. Med. Genet.* 154C, 377–386. doi: 10.1002/ajmg.c.30271
- Kfoury, Y., and Scadden, D. T. (2015). Mesenchymal cell contributions to the stem cell niche. *Cell Stem Cell* 16, 239–253. doi: 10.1016/j.stem.2015.02.019
- Klemke, M., Pasolli, H., Kehlenbach, R., Offermanns, S., Schultz, G., and Huttner, W. (2000). Characterization of the extra-large G protein alpha-subunit XL $\alpha$ phas. II. Signal transduction properties. *J. Biol. Chem.* 275, 33633–33640.
- Liu, J., Yu, S., Litman, D., Chen, W., and Weinstein, L. (2000). Identification of a methylation imprint mark within the mouse gnas locus. *Mol. Cell Biol.* 20, 5808–5817. doi: 10.1128/mcb.20.16.5808-5817.2000
- Mantovani, G., Spada, A., and Elli, F. M. (2016). Pseudohypoparathyroidism and G $\alpha$ ph $\alpha$ -cAMP-linked disorders: current view and open issues. *Nat. Rev. Endocrinol.* 12, 347–356. doi: 10.1038/nrendo.2016.52
- Mariot, V., Wu, J. Y., Aydin, C., Mantovani, G., Mahon, M. J., Linglart, A., et al. (2011). Potent constitutive cyclic AMP-generating activity of XL $\alpha$ phas implicates this imprinted GNAS product in the pathogenesis of McCune-Albright Syndrome and fibrous dysplasia of bone. *Bone* 48, 312–320. doi: 10.1016/j.bone.2010.09.032
- Michienzi, S., Cherman, N., Holmbeck, K., Funari, A., Collins, M. T., Bianco, P., et al. (2007). GNAS transcripts in skeletal progenitors: evidence for random asymmetric allelic expression of G $\alpha$ {alpha}. *Hum. Mol. Genet.* 16, 1921–1930. doi: 10.1093/hmg/ddm139
- Mulchandani, S., Bhoj, E. J., Luo, M., Powell-Hamilton, N., Jenny, K., Gripp, K. W., et al. (2016). Maternal uniparental disomy of chromosome 20: a novel imprinting disorder of growth failure. *Genet. Med.* 18, 309–315.
- Narumi, S., Matsuo, K., Ishii, T., Tanahashi, Y., and Hasegawa, T. (2013). Quantitative and sensitive detection of GNAS mutations causing mccune-albright syndrome with next generation sequencing. *PLoS One* 8:e60525. doi: 10.1371/journal.pone.0060525
- Pasolli, H. A., Klemke, M., Kehlenbach, R. H., Wang, Y., and Huttner, W. B. (2000). Characterization of the extra-large G protein alpha-subunit XL $\alpha$ phas. I. Tissue distribution and subcellular localization. *J. Biol. Chem.* 275, 33622–33632.
- Plagge, A., Gordon, E., Dean, W., Boiani, R., Cinti, S., Peters, J., et al. (2004). The imprinted signaling protein XL $\alpha$ phas is required for postnatal adaptation to feeding. *Nat. Genet.* 36, 818–826. doi: 10.1038/ng1397
- Plagge, A., Kelsey, G., and Germain-Lee, E. L. (2008). Physiological functions of the imprinted Gnas locus and its protein variants Galpha(s) and XL $\alpha$ pha(s) in human and mouse. *J. Endocrinol.* 196, 193–214. doi: 10.1677/joe-07-0544
- Richard, N., Molin, A., Coudray, N., Rault-Guillaume, P., Jüppner, H., and Kottler, M. L. (2013). Paternal GNAS mutations lead to severe intrauterine growth retardation (IUGR) and provide evidence for a role of XL $\alpha$ phas in fetal development. *J. Clin. Endocrinol. Metab.* 98, E1549–E1556.
- Roctus, A., Martin-Trujillo, A., Izzi, B., Elli, F., Garin, I., Linglart, A., et al. (2016). Genome-wide DNA methylation analysis of pseudohypoparathyroidism patients with GNAS imprinting defects. *Clin. Epigenetics* 8:10.
- Schwindinger, W. F., Francomano, C. A., and Levine, M. A. (1992). Identification of a mutation in the gene encoding the alpha subunit of the stimulatory G protein of adenyl cyclase in McCune-Albright syndrome. *Proc. Natl. Acad. Sci. U.S.A.* 89, 5152–5156. doi: 10.1073/pnas.89.11.5152
- Tafaj, O., Hann, S., Ayturk, U., Warman, M. L., and Juppner, H. (2017). Mice maintain predominantly maternal Galphas expression throughout life in brown fat tissue (BAT), but not other tissues. *Bone* 103, 177–187. doi: 10.1016/j.bone.2017.07.001
- Turan, S., Fernandez-Rebollo, E., Aydin, C., Zoto, T., Reyes, M., Bounoutas, G., et al. (2014). Postnatal establishment of allelic Galphas silencing as a plausible explanation for delayed onset of parathyroid hormone resistance owing to heterozygous Galphas disruption. *J. Bone Miner Res.* 29, 749–760. doi: 10.1002/jbmr.2070
- Weinstein, L. S., Liu, J., Sakamoto, A., Xie, T., and Chen, M. (2004). Minireview: GNAS: normal and abnormal functions. *Endocrinology* 145, 5459–5464. doi: 10.1210/en.2004-0865
- Weinstein, L. S., Shenker, A., Gejman, P. V., Merino, M. J., Friedman, E., and Spiegel, A. M. (1991). Activating mutations of the stimulatory G protein in the McCune-Albright syndrome. *New Engl. J. Med.* 325, 1688–1695. doi: 10.1056/nejm199112123252403
- Williamson, C. M., Ball, S. T., Dawson, C., Mehta, S., Beechey, C. V., Fray, M., et al. (2011). Uncoupling antisense-mediated silencing and DNA methylation in the imprinted Gnas cluster. *PLoS Genet.* 7:e1001347. doi: 10.1371/journal.pgen.1001347
- Williamson, C. M., Turner, M. D., Ball, S. T., Nottingham, W. T., Glenister, P., Fray, M., et al. (2006). Identification of an imprinting control region affecting the expression of all transcripts in the Gnas cluster. *Nat. Genet.* 38, 350–355. doi: 10.1038/ng1731
- Wu, J. Y., Aarnisalo, P., Bastepe, M., Sinha, P., Fulzele, K., Selig, M. K., et al. (2011). G $\alpha$ ph $\alpha$  enhances commitment of mesenchymal progenitors to the osteoblast lineage but restrains osteoblast differentiation in mice. *J. Clin. Invest.* 121, 3492–3504. doi: 10.1172/jci.46406
- Xiao, T., Fu, Y., Zhu, W., Xu, R., Xu, L., Zhang, P., et al. (2019). HDAC8, A potential therapeutic target, regulates proliferation and differentiation of bone marrow stromal cells in fibrous dysplasia. *Stem Cells Transl. Med.* 8, 148–161. doi: 10.1002/sctm.18-0057
- Yu, S., Yu, D., Lee, E., Eckhaus, M., Lee, R., Corria, Z., et al. (1998). Variable and tissue-specific hormone resistance in heterotrimeric G $\alpha$ s protein a-subunit (G $\alpha$ a) knockout mice is due to tissue-specific imprinting of the G $\alpha$ a gene. *Proc. Natl. Acad. Sci. U.S.A.* 95, 8715–8720. doi: 10.1073/pnas.95.15.8715

**Conflict of Interest:** The authors declare that the research was conducted in the absence of any commercial or financial relationships that could be construed as a potential conflict of interest.

Copyright © 2021 Cui, Aksu, Ay, Remillard, Plagge, Gardezi, Dunlap, Gerstenfeld, He and Bastepe. This is an open-access article distributed under the terms of the Creative Commons Attribution License (CC BY). The use, distribution or reproduction in other forums is permitted, provided the original author(s) and the copyright owner(s) are credited and that the original publication in this journal is cited, in accordance with accepted academic practice. No use, distribution or reproduction is permitted which does not comply with these terms.